The mixed longitudinal–transverse nature of collective modes in water

2010 New J. Phys. 12 053008

(http://iopscience.iop.org/1367-2630/12/5/053008)

New Journal of Physics
The open-access journal for physics

The mixed longitudinal–transverse nature of collective modes in water

A Cimatoribus[1,4], S Saccani[1,4], F Bencivenga[1], A Gessini[1], M G Izzo[1,2] and C Masciovecchio[1,3]

[1] Sincrotrone Trieste, 34149 Basovizza, Trieste, Italy
[2] Dipartimento di Fisica, Universitá degli Studi di Trieste, 34127 Trieste, Italy
[3] CRS SOFT-INFM-CNR, Universitá di Roma La Sapienza, 00185 Roma, Italy
E-mail: andrea.cimatoribus@gmail.com and sebastiano.saccani@gmail.com

New Journal of Physics **12** (2010) 053008 (10pp)
Received 2 December 2009
Published 6 May 2010
Online at http://www.njp.org/
doi:10.1088/1367-2630/12/5/053008

Abstract. We report high-resolution, high-statistics inelastic x-ray scattering measurements of the dynamic structure factor of water as a function of momentum and energy transfer in various thermodynamic conditions, including high-pressure liquid near the melting point, supercooled liquid and polycrystalline ice. For momentum transfer values below 8 nm^{-1}, two collective excitations associated with longitudinal and transverse acoustic modes were observed. Above 8 nm^{-1}, another excitation was detected in the liquid. Comparison with polycrystalline data and molecular dynamics simulations suggests that this mode is related to longitudinal–transverse mixing of mode symmetry.

Contents

[4] Authors to whom any correspondence should be addressed.

1. Introduction

Water is a system that has been widely studied because of its peculiar thermodynamic anomalies whose origin is not yet fully understood and because of its prominent role in several fields of applied and life sciences [1, 2]. One of the challenges that scientists are facing concerns the description of the high-frequency collective dynamics [3]–[17]. Notwithstanding the considerable amount of effort, a commonly accepted scenario is still missing.

The existence of a single longitudinal acoustic (LA) mode at low momentum transfer ($Q \lesssim 0.03\,\mathrm{nm}^{-1}$) has been demonstrated, propagating at a velocity equal to the adiabatic one (c_S) [18]. At higher Q values, a large increase of the speed of sound with respect to c_S (positive sound dispersion) is accompanied by the emergence of a weakly dispersive feature, at energies below the LA mode [6]. Whereas positive sound dispersion is fully accounted for by the viscoelastic theory of liquids [15, 19, 20], the nature of the second excitation is much more debated. At first, it was simply identified as the LA mode [3]. Molecular dynamics (MD) simulations showing the existence of this excitation date back to 1974 [21]. Later on, transverse optic nature was inferred based on inelastic x-ray scattering (IXS) experiments [6, 22] and further MD simulations [23]–[25]. Successive experimental and theoretical investigations pointed out the transverse acoustic (TA) character of this excitation [16, 26, 27]. Afterwards, the prevalent acoustic character of this mode was challenged again by neutron scattering experiments [10, 17].

Therefore, the first purpose of the present work is to identify the nature of the second excitation. To achieve this goal, we analyzed the lineshape of IXS spectra collected with an unprecedentedly high statistical accuracy in the region of exchanged momentum (Q) and energy ($\hbar\omega$) where the aforementioned phenomenology shows up. The sample was probed in different thermodynamic conditions, including the supercooled liquid phase, where experimental data on the high-frequency collective dynamics are lacking. IXS spectra of liquid and supercooled water were analyzed within the viscoelastic approach [19]. According to this framework, the dynamic response of the liquid is similar to that of the solid as long as the inverse structural relaxation time is much shorter than the frequencies of probed excitations. In the case of water, this condition is essentially met in the investigated thermodynamic range, particularly close to or below the melting point [6, 8, 9, 13]. Consequently, the analysis of IXS spectra from supercooled and polycrystalline water (the latter data were collected during the same experiment) in the same thermodynamic conditions allowed us to establish a closer comparison between the liquid and solid phases.

Our data were also compared to the literature results and allowed us to unambiguously assess the TA nature of this low-frequency mode (LFM) for $Q \leqslant Q_{MAX}/2$, where $Q_{MAX} \approx 8$–$9\,\mathrm{nm}^{-1}$ is the Q value corresponding to the first sharp diffraction peak in the static structure factor ($S(Q)$). Above Q_{MAX}, the prevalent TA nature of LFM cannot be decided anymore. Furthermore, a new high-frequency mode (HFM) is found in the liquid. We interpret this feature as likely due to intramolecular motions of mixed longitudinal–transverse symmetry. Even if we cannot exclude that the HFM has already been recorded in previous IXS experiments, its existence has never been reported. This is most likely due to the fact that the HFM is hardly discernible from the background in view of its very low cross section, and former investigators did not have the capability to analyze data of such high statistics, nor to study the supercooled liquid phase where, indeed, the HFM is slightly more evident.

Table 1. Thermodynamic point investigated in the present work. The probed Q-range and the employed sample environment were reported as well.

T (K)	P (Bar)	Q (nm^{-1})	Phase	Setup
263	1.2	2–18	Supercooled	Drop
263	1	2–14	Polycrystalline	Drop
263	3000	2–14	Liquid	HP
278	1	2–14	Liquid	HP
278	3000	2–14	Liquid	HP
288	3000	2–14	Liquid	HP
353	3000	2–14	Liquid	HP

2. Experimental setup and fitting procedure

Measurements were carried out at the IXS beamline (ID28) at the European Synchrotron Radiation Facility in Grenoble. ID28 was operated at the Si(11,11,11) configuration, delivering a total energy resolution of about 1.5 meV (full-width at half-maximum). Further details of the instrument can be found elsewhere [28]. The dynamical structure factor, $S(Q, \omega)$, was measured in the Q range of 2–18 nm^{-1} and in the $\hbar\omega$ range of $\pm$40 meV. The typical acquisition time for a set of IXS spectra was about 12–16 h. Table 1 reports the thermodynamic and kinematic points investigated in our experiment.

Two different sample environments were employed. The first one, suitable for undercooling, has been derived from a setup used for studying homogeneous nucleation [29] (Drop). In this case, the sample was a droplet of high-purity water of approximately 3 mm diameter. It was kept on a 100 μm-thick hydrophobic glass, sealed in a 5×2 cm^2 (diameter $\times$ height) chamber in a helium atmosphere at 1.2 bar, in order to prevent contamination from the atmosphere. This newly developed device prevented crystallization in the supercooled phase at 263 K for several hours, thus enabling IXS measurements. This apparatus was also used to collect data on polycrystalline ice I_h at the same temperature. The second setup is a high-pressure (HP) apparatus already used to carry out several IXS experiments [8, 16, 30].

Data were analyzed using the viscoelastic approach [19], which has already been successfully employed in the interpretation of high-frequency dynamics of liquid water and other liquids [8, 9, 13, 16, 19, 30, 31]. The expression for $S(Q, \omega)$ can be obtained within the memory function formalism. Memory function theory is used to derive a generalized Langevin equation for the density correlation function, $F(Q, t)$:

$$\frac{\partial^2 F(Q,t)}{\partial t^2} + \omega_0^2 F(Q,t) + \int_0^t m(Q, t-t') \frac{\partial F(Q,t')}{\partial t'} \mathrm{d}t' = 0, \tag{1}$$

where ω_0 is the frequency of sound excitation in the hydrodynamic ($Q \to 0$) limit and $m(t)$ is the memory function. The Fourier transform of $F(Q, t)$, i.e. $S(Q, \omega)$, then reads:

$$\frac{S(Q,\omega)}{S(Q)} = \frac{1}{\pi} \frac{\omega_0^2 M'(Q,\omega)}{[\omega_0^2 - \omega^2 - \omega M''(Q,\omega)]^2 + [\omega M'(Q,\omega)]^2}, \tag{2}$$

where $M'(Q,\omega)$ and $M''(Q,\omega)$ are the real and imaginary parts of the Fourier transform of $m(Q,t)$. In the case of water, $m(Q,t)$ can be approximated as [8, 13, 16]:

$$m(Q,t) = (\gamma(Q)-1)(c_t(Q)Q)^2 e^{-D_T(Q)Q^2 t} + \Delta_\alpha(Q)^2(Q)e^{-t/\tau_\alpha(Q)} + 2\Gamma_\mu(Q)\delta(t). \quad (3)$$

In the first term on the right-hand side of (3), $c_t(Q)$, $\gamma(Q)$ and $D_T(Q)$ are the Q-dependent generalizations of the isothermal speed of sound, specific heats ratio and thermal conductivity, respectively. In the second term on the right-hand side of (3), $\Delta_\alpha(Q)$ and $\tau_\alpha(Q)$ are the structural relaxation strength and time, while in the third term, $\Gamma_\mu(Q)$ represents the strength of the instantaneous relaxation [8, 9, 13, 16, 19]. It is also useful to introduce the LA frequency in the elastic regime: $\omega_\infty = \sqrt{\omega_0^2 + \Delta_\alpha^2}$. In order to account for the aforementioned weakly dispersive LFM and HFM, we added two damped harmonic oscillator (DHO) functions, following the idea of [16]:

$$S(Q,\omega) = \frac{I_L}{\pi}\frac{\omega_0^2 M'(Q,\omega)}{[\omega_0^2-\omega^2-\omega M''(Q,\omega)]^2+[\omega M'(Q,\omega)]^2} + I_T\frac{\Omega_T^2\Gamma_T}{(\Omega_T^2-\omega^2)^2+(\omega\Gamma_T)^2} + I_{HFM}\frac{\Omega_{HFM}^2\Gamma_{HFM}}{(\Omega_{HFM}^2-\omega^2)^2+(\omega\Gamma_{HFM})^2}, \quad (4)$$

where Ω_T and Γ_T are the characteristic frequency and damping of LFM, while I_T and I_L are scaling factors. For $Q \geqslant 8\,\mathrm{nm}^{-1}$, we were able to detect the HFM, empirically accounted for in the model function by adding a further DHO function, denoted in (4) by the suffix 'HFM'. The resulting $S(Q,\omega)$ has to be multiplied by the weighting factor:

$$w(\omega,T) = \frac{\hbar\omega}{k_b T}[1-e^{-\hbar\omega/k_b T}]^{-1} \quad (5)$$

in order to account for occupation of the different vibrational levels. Finally, a convolution with the experimental resolution function ($R(\omega)$) and the addition of a flat background (B) are needed to obtain the complete fitting function:

$$I(Q,\omega) = R(\omega)\otimes[w(\omega,T)\times S(Q,\omega)] + B. \quad (6)$$

Fits are based on χ^2 minimization; the description of the experimental data was always good, with reliability better than 0.99. It must be stressed that all lineshape parameters were always left free to vary without constraints. The results using the model currently described are consistent with those from a model with three DHOs.

In figure 1, selected IXS spectra of polycrystalline and liquid water are shown on a logarithmic scale, together with the corresponding best fit results. In the liquid, besides the dominant LA mode, we observe that the low-energy excitation is properly fitted (figure 1, middle and bottom panels). Above $8\,\mathrm{nm}^{-1}$, the new HFM is visible at $\approx 30\,\mathrm{meV}$. This excitation has never been experimentally observed before and is present both in the supercooled phase and in the HP liquid above the melting point. In the spectra from the polycrystal, in the first pseudo-Brillouin zone (BZ) (top right) a single LFM is observed below the dominant LA branch. In the second pseudo-BZ (top center and left), a double LFM feature is evident. Moreover, at larger energy transfers, the relic of the LA branch is accompanied by the rise of a new HFM in the range 30–35 meV.

To support the consistency of the analysis based on (4), data above $Q \approx 8\,\mathrm{nm}^{-1}$ were also fitted without the HFM term. As far as the viscoelastic parameters are concerned, both approaches give very similar results. The major difference found was in the parameter ω_0, which

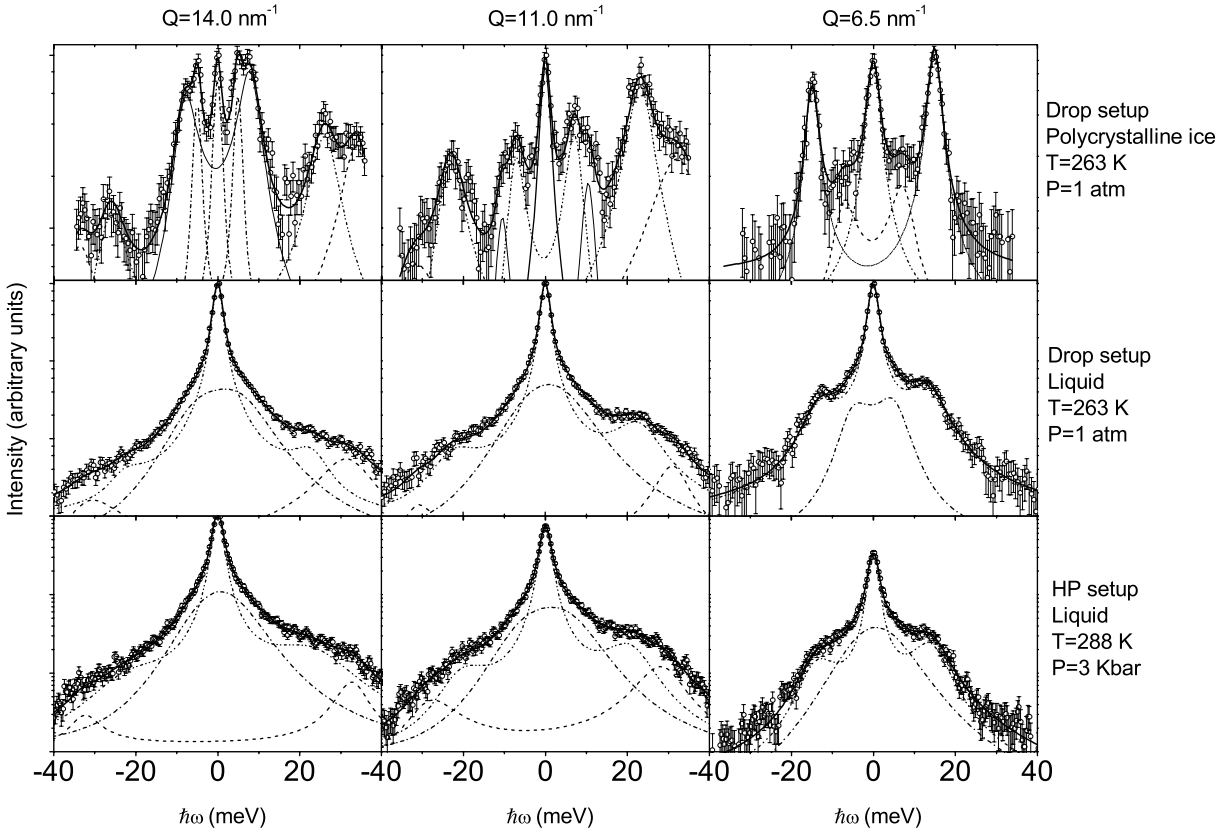

Figure 1. Representative IXS spectra from polycrystalline ice at $T = 263\,\mathrm{K}$ (top panels), from supercooled liquid water at $T = 263\,\mathrm{K}$ ('drop' setup, medium panels) and from liquid water at $P = 3\,\mathrm{kbar}$ and $T = 288\,\mathrm{K}$ ('HP' setup, bottom panels), at $Q = 6.5\,\mathrm{nm}^{-1}$ (left panels), $11\,\mathrm{nm}^{-1}$ (central panels) and $14\,\mathrm{nm}^{-1}$ (right panels). Empty circles are experimental data; the thick solid line is the best fit results. The dash–dot–dot line is the viscoelastic function accounting for LA and quasi-elastic contributions. The dash–dot line marks low-energy modes and the dashed line is a newly observed high-energy excitation.

is somewhat smaller. To investigate this difference, we compared the obtained results with the expected trend, i.e.

$$\omega_0(Q, T, P) = \frac{c_s(T, P)Q}{\sqrt{S(Q)/S(Q=0)}}, \tag{7}$$

where c_s is the adiabatic speed of sound, calculated from the well-known equation of state of water, whereas $S(Q)$ was measured contextually to the same experiment directly using the ID28 spectrometer. We observe that (4) with the HFM term gave slightly more consistent results, as can be appreciated by inspecting figure 2, which reports the case of water at 278 K and 3 kbar.

3. Experimental results

The left panels of figure 3 report the Q-dispersion relation of characteristic frequencies of the various modes, as extracted from IXS spectra using (4). In order to compensate for differences

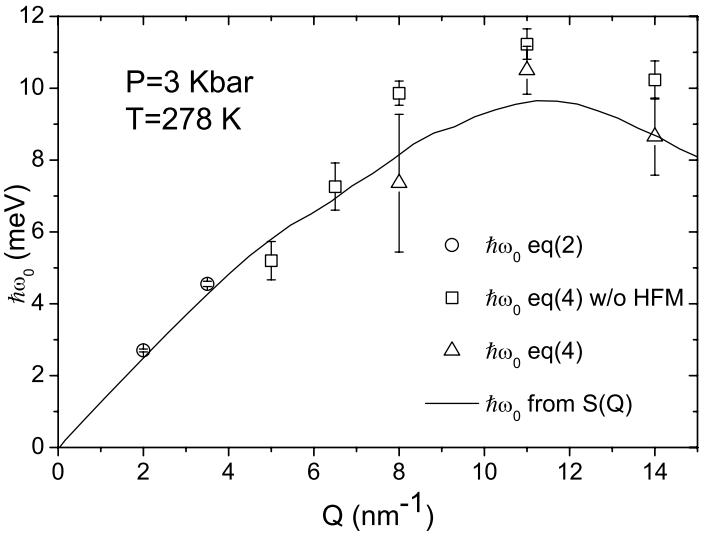

Figure 2. Values of ω_0 obtained employing equation (2) for $Q < 4\,\mathrm{nm}^{-1}$ and (4) without the HFM term above this value (squares). Results from (4) with the HFM contribution (triangles) for $Q \geqslant 8\,\mathrm{nm}^{-1}$ are plotted as well. The solid line is the expected ω_0 trend, calculated from $S(Q)$.

in density, the Q-axis was normalized by the measured value of Q_{MAX}[5]. In the panel referring to the supercooled liquid, the solid line is the $Q = 0$ extrapolation of sound velocity obtained from a sine fit of LFM for $Q < 12\,\mathrm{nm}^{-1}$, which gives $c_{\mathrm{LFM}} = 1800 \pm 100\,\mathrm{m\,s}^{-1}$. This estimate of the sound velocity for the LFM in the supercooled case is just below the transverse sound velocity of the polycrystal, calculated from both the Voigt ($1947\,\mathrm{m\,s}^{-1}$) and Reuss ($1965\,\mathrm{m\,s}^{-1}$) averages [33, 34]. In the calculation, elastic constants measured by Stephens [35] were used. Furthermore, the LFM in the liquid follows the expected dispersion for an acoustic mode, that is, $\omega(Q) \propto Q \times S(Q)^{-1/2}$ [19]. In the right panels of figure 3, the vibrational density of states (DoS) from neutron scattering measurements [11] is displayed. The analysis made by the authors revealed that the energy regions characteristic of LFM (in 8–14 meV) in the DoS of the polycrystal can be unambiguously assigned as arising from acoustic modes [11]. Therefore, the comparison between neutron scattering results and the water and polycrystalline data strongly supports the TA nature of LFM up to $Q/Q_{\mathrm{MAX}} \approx 0.4$.

Moreover, the almost flat dispersion and large intensity of LFM are consistent with the main peak in the DoS, while the intensity decrease of the LA mode at large E is consistent with the plateau between 13 and 27 meV. Similarly, the feature at 25 meV reflects the dispersiveless behavior of the LA branch at high Q.

Finally, a comparison of supercooled water data, which are the most sampled dataset, with previous MD simulations is shown in figure 4. The characteristic energies of longitudinal (+) and transverse ($\times$) current correlation functions [27] are displayed. The analogy suggests that the observed LFM is a projection of the transverse current correlation function onto the longitudinal one (see figure 4, bottom panel). In light of these pieces of evidence, we can reasonably conclude that the LFM has a TA nature also in the liquid below $8\,\mathrm{nm}^{-1}$. In addition, at higher Q values, MD results highlight the rise of an LFM in the longitudinal current spectrum too.

[5] In the case of the polycrystalline sample, Q_{MAX} is from [32].

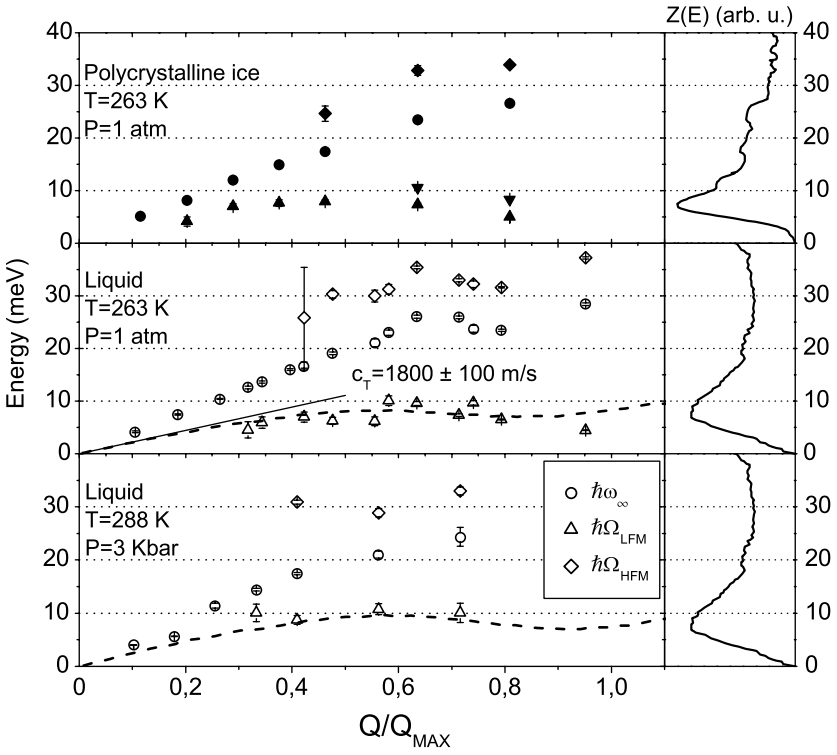

Figure 3. Dispersion of the modes as a function of Q/Q_{MAX}. Full symbols refer to the polycrystal, whereas empty symbols refer to the liquid. On the right part of every panel, DoS on the polycrystal ($Z(E)$) at 270 K and on the liquid at 280 K are displayed, as measured by Dawidowski *et al* [11]. The branches structure is analogous in the polycrystal and the liquid and is not affected by the sample environment. In the panel referring to the supercooled liquid, the solid line is the extrapolation of TA sound velocity in the $Q = 0$ limit. Dashed lines are proportional to $Q \times S(Q)^{-1/2}$ (see text).

However, being almost degenerate with TA modes, the two branches cannot be experimentally discriminated.

Above $Q/Q_{\mathrm{MAX}} \approx 0.4$, the HFM appears in the spectra from the liquid. The rather large dispersion of experimental data together with the impossibility to determine the HFM frequencies at low Q do not allow the unambiguous identification of the Q-dispersion relation of such a mode. Therefore, an acoustic or optic-like nature cannot be discriminated on such grounds. However, closer comparison of our data with the DoS reveals that similar vibrational modes are present also in the polycrystal in this energy range. It has been noted that the features of DoS in the polycrystal between 20 and 40 meV are generally discussed in terms of molecular optic modes [11]. In view of the strong analogies mentioned above, it is straightforward to assume that also a mode involving intramolecular motion has a strong resemblance in the liquid and the polycrystal. This holds in particular considering the lack of long-range order of protons in ice I_{h}. Consequently, the HFMs in the liquid should probably be regarded as being of mostly molecular optic nature as well, even though the limited Q range explored in the present work confines the conclusions to qualitative arguments. Looking at the top panel of figure 4, it can

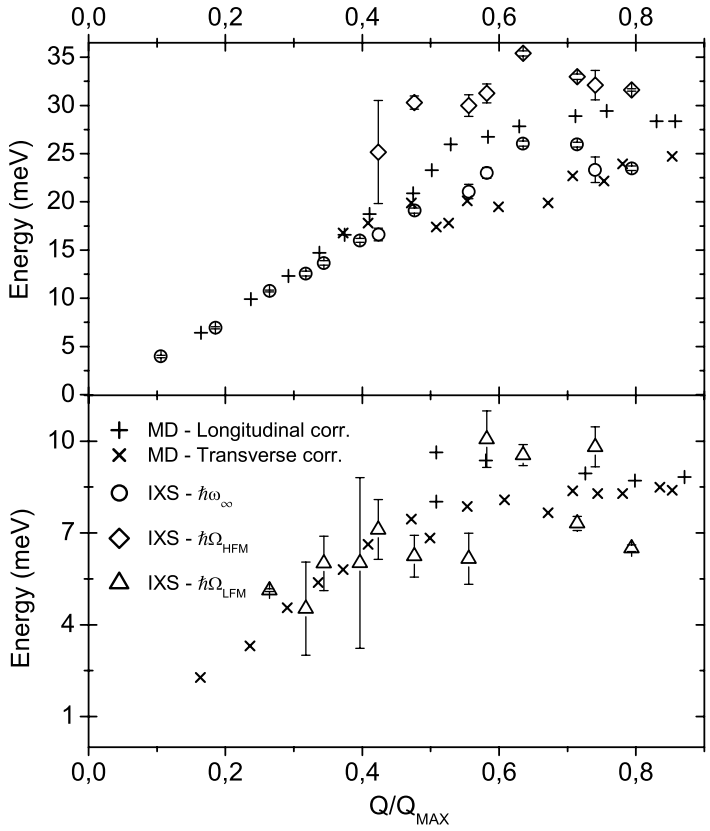

Figure 4. Q-dispersion of inelastic excitations observed in the supercooled liquid from experiment (empty symbols) and simulations [27] (+ and ×). The top and bottom panels display HFMs and LFMs, respectively.

be noted that the experimentally detected HFM rises at the same Q/Q_{MAX} value where an excitation of similar energy appears in the simulated transverse current correlation function. Thus, it is straightforward to hypothesize that the measured HFM can be ascribed to a projection of the transverse current correlation on the $S(Q, E)$. Moreover, energy separation between HFM and LA branches from the experiment is very close to MD results. The existence of multiple peaks at high Q values is also supported by other simulations [26], carried out using a different intermolecular potential.

4. Conclusions

We reported on and discussed new high-resolution IXS data on water in various thermodynamic conditions, including the supercooled liquid and polycrystalline phases. We provided some evidence of the TA nature of the mode observed in liquid water at frequencies below the dominant LA branch. Above $\approx 8\,\mathrm{nm}^{-1}$, we observed a new high-frequency excitation in the liquid phase. It is likely related to intramolecular dynamics and reflects crystalline-like dynamics of the prevalent optic nature. Comparison with MD simulations allows us to assess whether its origin is connected with the transverse current correlation function. The appearance in the density fluctuation spectrum of features from the transverse current correlation function

fingerprints the mixed longitudinal–transverse nature of microscopic dynamics in water at short wavelengths, and its general resemblance to crystalline dynamics. Since liquids usually show a single branch associated with LA modes, the appearance of multiple excitation branches is likely associated with transverse and longitudinal correlations. This may be a novel manifestation of the unique water structure. Further experimental efforts, aimed at probing dynamics in systems with a water-like local intermolecular structure, are in progress and may shed new light on this topic.

Acknowledgments

We acknowledge Dr Jorge Serrano and Dr Roberto Verbeni for their valuable help during the IXS experiment. CM acknowledges support from the European Research Council under the European Community Seventh Framework Program (FP7/2007-2013)/ERC IDEAS contract no. 202804.

References

[1] Mishima O and Stanley H E 1998 The relationship between liquid, supercooled and glassy water *Nature* **396** 329
[2] Angell C A 1981 *Water: A Comprehensive Treatise* vol 7 (New York: Plenum)
[3] Bosi P, Dupré F, Menzinger F, Sacchetti F and Spinelli M C 1978 Observation of collective excitations in heavy water in the 10^8 cm^{-1} momentum range *Nuovo Cimento Lett.* **21** 436
[4] Teixeira J, Bellissent-Funel M C, Chen S H and Dorner B 1985 Observation of new short-wavelength collective excitations in heavy water by coherent inelastic neutron scattering *Phys. Rev. Lett.* **54** 2681
[5] Ruocco G, Sette F, Bergmann U, Krisch M, Masciovecchio C, Mazzacurati V, Signorelli G and Verbeni R 1996 Equivalence of the sound velocity in water and ice at mesoscopic wavelengths *Nature* **379** 521
[6] Sette F, Ruocco G, Krisch M, Masciovecchio C, Verbeni R and Bergmann U 1996 Transition from normal to fast sound in liquid water *Phys. Rev. Lett.* **77** 83
[7] Sette F, Ruocco G, Krisch M, Masciovecchio C and Verbeni R 1996 Collective dynamics in water by inelastic x-rays scattering *Phys. Scr.* T **66** 48–56
[8] Monaco G, Cunsolo A, Ruocco G and Sette F 1999 Viscoelastic behavior of water in the terahertz-frequency range: an inelastic x-ray scattering study *Phys. Rev.* E **60** 5505
[9] Cunsolo A, Ruocco G, Sette F, Masciovecchio C, Mermet A, Monaco G, Sampoli M and Verbeni R 1999 Experimental determination of the structural relaxation in liquid water *Phys. Rev. Lett.* **82** 775
[10] Petrillo C, Sacchetti F, Dorner B and Suck J-B 2000 High-resolution neutron scattering measurement of the dynamic structure factor of heavy water *Phys. Rev.* E **62** 3611
[11] Dawidowski J, Bermejo F J, Cabrillo C and Bennington S M 2000 Generalized frequency spectra of water at both sides of the freezing transition *Chem. Phys.* **258** 247
[12] Masciovecchio C, Santucci S C, Gessini A, Di Fonzo S, Ruocco G and Sette F 2004 Structural relaxation in liquid water by inelastic UV scattering *Phys. Rev. Lett.* **92** 255507
[13] Bencivenga F, Cunsolo A, Krisch M, Monaco G, Ruocco G and Sette F 2007 High-frequency dynamics of liquid and supercritical water *Phys. Rev.* E **75** 051202
[14] Bencivenga F, Cimatoribus A, Gessini A, Izzo M G and Masciovecchio C 2009 Temperature and density dependence of the structural relaxation time in water by inelastic ultraviolet scattering *J. Chem. Phys.* **131** 144502
[15] Santucci S C, Fioretto D, Comez L, Gessini A and Masciovecchio C 2006 Is there any fast sound in water? *Phys. Rev. Lett.* **97** 225701

[16] Pontecorvo E, Krisch M, Cunsolo A, Monaco G, Mermet A, Verbeni R, Sette F and Ruocco G 2005 High-frequency longitudinal and transverse dynamics in water *Phys. Rev.* E **71** 011501
[17] Sacchetti F, Suck J-B, Petrillo C and Dorner B 2004 Brillouin neutron scattering in heavy water: evidence for two-mode collective dynamics *Phys. Rev.* E **69** 061203
[18] Berne B J and Pecora R 2000 *Dynamic Light Scattering with Applications to Chemistry, Biology and Physics* (Mineola, NY: Dover)
[19] Boon J P and Yip S 1991 *Molecular Hydrodynamics* (Mineola, NY: Dover)
[20] Huang K 1987 *Statistical Mechanics* (New York: Wiley)
[21] Rahman A and Stillinger F H 1974 Propagation of sound in water. a molecular-dynamics study *Phys. Rev.* A **10** 368
[22] Tozzini V and Tosi M P 1996 Viscoelastic model for the transition from normal to fast sound in water *Phys. Chem. Liq.* **33** 191
[23] Ricci M A, Rocca D, Ruocco G and Vallauri R 1988 Collective dynamical properties of liquid water *Phys. Rev. Lett.* **61** 1958
[24] Sastry S, Sciortino F and Stanley H E 1991 Collective excitations in liquid water at low frequency and large wave vector *J. Chem. Phys.* **95** 7775
[25] Bertolini D and Tani A 1995 Generalized hydrodynamics and the acoustic modes of water: theory and simulation results *Phys. Rev.* E **51** 1091
[26] Sampoli M, Ruocco G and Sette F 1997 Mixing of longitudinal and transverse dynamics in liquid water *Phys. Rev. Lett.* **79** 1678
[27] Balucani U, Brodholt J P and Vallauri R 1996 Dynamical properties of liquid water *J. Phys.: Condens. Matter* **8** 9269
[28] Krisch M 2003 Status of phonon studies at high pressure by inelastic x-ray scattering *J. Raman Spectrosc.* **34** 628
[29] Seeley L H, Seidler G T and Dash J G 1999 Apparatus for statistical studies of heterogeneous nucleation *Rev. Sci. Instrum.* **70** 3664
[30] Bencivenga F, Cunsolo A, Krisch M, Monaco G, Ruocco G and Sette F 2009 High frequency dynamics in liquids and supercritical fluids: a comparative inelastic x-ray scattering study *J. Chem. Phys.* **130** 064501
[31] Bencivenga F, Cunsolo A, Krisch M, Monaco G, Orsingher L, Ruocco G, Sette F and Vispa A 2007 Structural and collisional relaxations in liquids and supercritical fluids *Phys. Rev. Lett.* **98** 085501
[32] Bermejo F J, Frikkee E, Garcia-Hernandez M, Martinez J L and Criado A 1993 Neutron scattering from polycrystalline ice (ih): some keys to understanding the collective behavior of liquid water *Phys. Rev.* E **48** 2300
[33] Antonangeli D, Krisch M, Fiquet G, Badro J, Farber D L, Bossak A and Merkel S 2005 Aggregate and single-crystalline elasticity of hcp cobalt at high pressure *Phys. Rev.* B **72** 134303
[34] Ashcroft N W and Mermin N D 1976 *Solid State Physics* (Philadelphia, PA: Saunders)
[35] Stephens R W B 1958 The mechanical properties of ice. II. The elastic constants and mechanical relaxation of single crystal ice *Adv. Phys.* **7** 266